MR Fat Fraction Mapping:

A Simple Biomarker for Liver Steatosis Quantification in Nonalcoholic Fatty Liver Disease Patients

Helena S. Leitão, MD, Cláudia Paulino, MD, Dírcea Rodrigues, MD, Sónia I. Gonçalves, PhD, Cristina Marques, MD, Manuela Carvalheiro, MD, PhD, Carlos F. G. C. Geraldes, PhD, Filipe Caseiro-Alves, MD, PhD

Rationale and Objectives: To assess the performance, postprocessing time, and intra- and interobserver agreement of a simple magnetic resonance–based mapping technique to quantify liver fat.

Materials and Methods: This prospective, single-center study included 26 patients who were overweight with type 2 diabetes and at risk for nonalcoholic fatty liver disease. Mapping of the liver was based on a triple echo gradient-echo sequence, and ^{1}H magnetic resonance spectroscopy was used as the reference standard. The nonparametric Spearman correlation coefficient and the Wilcoxon test were used for comparisons between mapping and spectroscopy. The mapping was assessed for its predictive performance using the area under the curve of a receiver operating characteristic curve. Intraclass correlation coefficients were used to calculate intra- and interobserver's agreement for mapping measurements.

Results: Patients had a mean fat percentage of 11.7% (range, 2–35.4%). A strong correlation was seen between mapping and spectroscopy (r = 0.89, P < .0001). A cutoff of 6.9% for fat fraction mapping was found to diagnose steatosis with 93% sensitivity and 100% specificity with an area under the curve of 0.99. Mapping of the liver had shorter acquisition and post-processing times than spectroscopy (5 min vs. 38 min; P < .0001). Mapping measurements had an intra- and interobserver agreement of 0.98 and 0.99, respectively.

Conclusions: The magnetic resonance–based liver mapping can accurately quantify liver fat with a cutoff value of 6.9% and excellent intra- and interobserver agreement. This mapping technique, with its simple methodology and short postprocessing time, has the potential to be included in routine abdominal protocols.

Key Words: Magnetic resonance imaging; magnetic resonance spectroscopy; fatty liver disease; mapping; fat quantification.

Nonalcoholic fatty liver disease is being increasingly recognized as a disease associated to liver-related morbidity and even mortality in the western countries. Its prevalence has been rising in the past two decades to become the leading cause of chronic liver disease, being closely associated to insulin resistance and type 2 diabetes (1,2). This chronic liver disease includes not only bland steatosis but also steatohepatitis, which can progress to fibrosis, cirrhosis, and ultimately hepatocellular carcinoma (2). Although early stages of liver steatosis may be reversible, patients can progress to nonalcoholic steatohepatitis even without any proven inflammation or cell injury (3–6). Liver biopsy is the current gold standard for diagnosing nonalcoholic fatty liver disease and quantifying liver fat. However, its invasive nature limits the use for screening or follow-up of nonalcoholic fatty liver disease patients (7). Alternative noninvasive imaging methods, such as magnetic resonance spectroscopy (MRS) and multiecho (≥6 echos) gradient-echo imaging with or without fat spectral modeling, have been used to accurately quantify liver fat (8–12). However, they are time-consuming and require the use of extensive logarithmic calculations. Yokoo et al (9,10) have recently found no significant differences between triple echo gradient-echo imaging and the more complex methods for fat quantification. Therefore, the purpose of our study was to 1) assess the performance and specific cutoff value of a simple MR-based mapping technique for liver fat quantification at 1.5-T in patients at risk for nonalcoholic fatty liver disease, 2) quantify the time it can add to routine clinical practice abdominal protocols and 3) assess its intra- and interobserver reproducibility.

Acad Radiol 2013; 20:957–961

From the Center for Neuroscience and Cell Biology, PhD Program in Experimental Biology and Biomedicine, University of Coimbra, Coimbra, Portugal (H.S.L., C.F.G.C.G.); University Clinic of Radiology, Coimbra University Hospitals, Coimbra, Portugal (H.S.L. C.P., S.I.G., C.M., F.C.-A.); Faculty of Medicine, University of Coimbra, Coimbra, Portugal (H.S.L., F.C.-A.); Department of Endocrinology, Diabetes and Metabolism, Coimbra University Hospitals, Coimbra, Portugal (D.R., M.C.); Department of Life Sciences, Faculty of Science and Technology, and Coimbra Chemistry Center, University of Coimbra, Coimbra, Portugal (C.F.G.C.G.). Received March 11, 2013; accepted May 7, 2013. H.S.L. received a grant (SFRH/BD/33893/2009) from the Foundation for Science and Technology (Portugal). **Address correspondence to:** H.S.L. e-mail: helenasleitao@zonmail.pt

http://dx.doi.org/10.1016/j.acra.2013.05.004

MATERIALS AND METHODS

Study Design and Patients

This prospective, single-center study was approved by the review board at our institution and written informed consent was obtained for all patients. Between May 2010 and June 2011, a screening program was initiated at the department of endocrinology using the following inclusion criteria: age 18 years and older, overweight with type 2 diabetes, at risk for nonalcoholic fatty liver disease, and absence of a clinical history or biochemical data consistent with hepatitis, cirrhosis, or hemochromatosis. A total of 32 patients were initially included in the study protocol that consisted of liver MR imaging at 1.5-T (Magnetom Symphony, Siemens Healthcare, Erlangen, Germany), using a four-element surface coil, performing triple echo gradient-echo T1-weighted MR imaging, from which the fat fraction mapping was processed, and ^{1}H MRS, used as the reference standard. Six patients were excluded for the following reasons: two patients because of technical failure during the MRS acquisition, two had uninterpretable spectra, and two missed the scheduled MR imaging. The final study population consisted of 26 patients, 6 men and 20 women, with a mean age of 47 years (range, 28–70 for women; 25–55 years for men). The mean body mass index was 36.2 kg/m^2 (range, 25–44 kg/m^2 for women; 33–48 kg/m^2 for men).

Magnetic Resonance Imaging

^{1}H MRS. Single-voxel liver spectroscopy was performed with a 30 mm × 30 mm × 30 mm voxel (27 mL). Spectra were acquired with the use of point-resolved spectroscopy sequence during free breathing. Water suppression was not performed. To minimize T1 effects, repetition time was set at 3000 ms. To correct for T2 effects, five average spectra were collected at echo times 20, 30, 40, 50, 60, and 80 ms. Other parameters were receiver bandwidth 2000 Hz and 2048 point spectral resolution. Automated optimization of gradient shimming was followed by manual adjustment of the central frequency, and spectra were used only if full width at half maximum water peak was 40 Hz or less. The total acquisition time was 3 minutes, 6 seconds. A region of interest containing a tissue volume of 27 mL was placed in one segment of the right liver at least 10 mm from the edge of the liver, avoiding vessels or focal lesions, by a radiologist with 5 years of experience in MR abdominal imaging. The ^{1}H MRS data were analyzed with the spectroscopic analysis package jMRUI (A. van den Boogaart, Catholic University, Leuven, Belgium). We measured the water peak (H_2O) at 4.7 ppm and the methylene peak (CH_2) at 1.3 ppm (13). T2 relaxation for water and methylene were determined from their integral values, at each echo time, by using a standard least-squares fitting algorithm with the following equation (12):

$$A(t) = A_0 \cdot e^{(-t/T2)} \quad [1]$$

where A is the integral value at time t and A_0 is the integral value at time 0.

The peak areas of water and methylene corrected for T2 effects ($A_{0\ H2O}$ and $A_{0\ CH2}$) were used to calculate liver fat fraction with the following equation (12):

$$\%FF = 100 \cdot A_{0\ CH2}/(A_{0\ CH2} + A_{0\ H2O})$$

We used the 5.56% value proposed by Szczepaniak et al (8), as a threshold for the upper normal limit of liver fat. Time required for postprocessing the MRS data were registered in each patient.

Fat fraction mapping (FFM). A T1-weighted two-dimensional triple echo gradient-echo sequence was initially acquired with a repetition time/echo time 164/4.6 ms (in phase$_1$, IP$_1$), 7.27 ms (opposed phase, OP), 9.98 ms (in phase$_2$, IP$_2$), matrix 192 × 256 pixels, 390 mm field of view (providing a pixel size of 2.0 × 1.5 mm), slice thickness 6 mm, and 20° flip angle to correct for the T1-weighting effect. The acquisition time was 35 seconds. The final liver fat fraction mapping images were acquired on an automated pixel-by-pixel basis and computed in a postprocessing workstation (Leonardo, Siemens Healthcare, Erlangen, Germany) using its basic mathematical functions as follows: 1) images representing the IP signal intensity (SI) were corrected for T2* decay (SI_{IPco}) using the arithmetic mean function, where $SI_{IPco} = (IP_1 + IP_2)/2$; 2) OP images ($SI_{OP}$) were subtracted from the previously obtained SI_{IPco} images ($SI_{IPco} - SI_{OP}$); 3) the final fat fraction mapping images were obtained by dividing the ($SI_{IPco} - SI_{OP}$) images by SI_{IPco} images, and applying a scaling factor of 50%, as previously reported (14). A circular region of interest of 2–3 cm^2 was manually placed by a radiologist blinded to spectroscopy results at the right liver lobe, visually matching the anatomical location of the spectroscopic region of interest and avoiding vessels or focal lesions. The region of interest drawn in the liver mapping provided an immediate percentage result of the fat content in that area (Figs 1 and 2). A similar volume-matched region of interest was placed in the spleen to serve as internal reference for technical consistency. All FFM were repeated 1 week later to assess intraobserver reproducibility by a radiologist with 5-year experience in MR abdominal imaging. Ten cases were randomly selected to assess interobserver reproducibility, which was performed by one radiologist with 2-year experience in MR abdominal imaging. The latter was previously taught to postprocess the IP/OP images to obtain the fat fraction mapping in half an hour. Time required for postprocessing the FFM was registered for each patient.

Statistical analysis. In this prospective study an a priori power analysis was performed to obtain a significance of 0.05 and a power of at least 80%. Previous reports in the literature for the prevalence of liver steatosis and mean liver fat content in a similar population were used for that purpose (11,15).

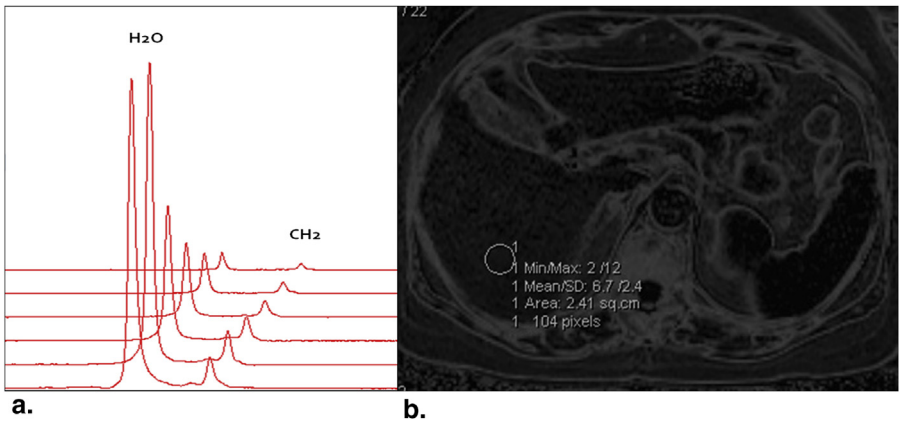

Figure 1. **(a)** ^{1}H magnetic resonance spectra and **(b)** liver fat fraction mapping of a 67-year-old patient with type 2 diabetes. **(a)** Liver fat content was 5.7%. **(b)** Region of interest (1) positioned in the liver directly provides the respective fat fraction value of 6.7%. Liver signal is only slightly more intense compared to the spleen (internal reference standard).

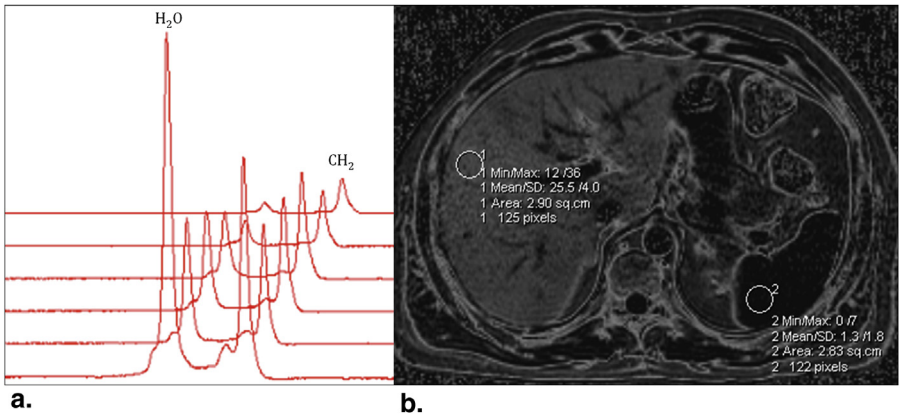

Figure 2. **(a)** ^{1}H magnetic resonance spectra and **(b)** liver fat fraction mapping of a 40-year-old patient with type 2 diabetes and severe steatosis. **(a)** Liver fat content was 26.7%. **(b)** Liver fat is clearly visible on the mapping, as the liver is hyperintense compared to the spleen. Measurements in the liver (1) and spleen (2) provide fat fraction within regions of interest (25.5% and 1.3%, respectively).

A minimum number of 21 patients had to be included in our study.

The correlation between the FFM measurements and MRS was assessed using the nonparametric Spearman rank correlation coefficient (r). The evaluation of bias was done using the 95% limit-of-agreement method developed by Bland and Altman (16), in which the difference between fat content measured by two methods is plotted against their mean. The performance of the fat fraction mapping was assessed by plotting the true-positive rate in function of the false-positive rate for different cutoff points, which allowed calculating the area under the curve of a receiver operating characteristic curve and determining the cutoff value for the technique. The difference in acquisition and postprocessing times between both methods was assessed using the nonparametric Wilcoxon test. Intra- and interobserver reproducibility was calculated using intraclass correlation coefficients. A P value $\leq .05$ was considered statistically significant. Statistical analysis was performed with the MedCalc software (MedCalc, Mariakerke, Belgium) and GraphPad software (GraphPad, San Diego, CA).

RESULTS

In this patient cohort a mean fat percentage of 11.7% (range, 2–35.4%) was obtained using the FFM technique corresponding to 9.8% (range, 0.8–30%) using MRS (Table 1). A strong correlation was found between both methods ($r = 0.89$, $P < .0001$). On the Bland-Altman plot, 25 of the 26 fat measurements were within ±4.2% of the mean difference of both methods (2%) (Fig 3). Using the reference threshold proposed by Szczepaniak et al (8) for MRS, we found that a cutoff value of 6.9% for FFM provided an accurate diagnosis of fat content with 93% sensitivity and 100% specificity. The area under the curve for FFM was 0.99. The spleen was used as our internal reference and all spleen measurements had a fat content ≤1.5% (Fig 2). Median postprocessing and reading time was 5 minutes (range, 5–15 minutes) for FFM and 35 minutes (range, 30–50 minutes) for MRS ($P < .0001$). Intraclass correlation coefficients for intra- and interobserver agreement were 0.98 (95% CI, 0.96–0.99) and 0.99 (95% CI, 0.97–0.99), respectively.

DISCUSSION

In this prospective, single-center study, we have assessed the performance, postprocessing time, and intra- and interobserver agreement of an MR-based mapping for liver fat quantification using a triple-echo gradient-echo sequence for T2⋆ correction. Our results show that this mapping can accurately provide liver fat quantification

TABLE 1. Fat Fraction Measurements with FFM and MRS in the 26 Patients

Fat Fraction Mapping (%)	Magnetic Resonance Spectroscopy (%)
4.8	1.2
2.8	0.8
2.6	0.8
27.4	28.6
4.5	1.2
35.4	30
15.7	14.2
2.0	1.0
6.7	5.7
12.0	7.0
15.9	15
10.8	7.3
3.0	1.0
20.8	21.7
25.5	26.7
12.6	10.8
6.9	3.1
2.5	1.0
5.3	1.3
11.4	10.3
16.8	20.5
6.7	1.6
2.2	0.8
6.8	4.4
31.7	29.3
12.0	11.0

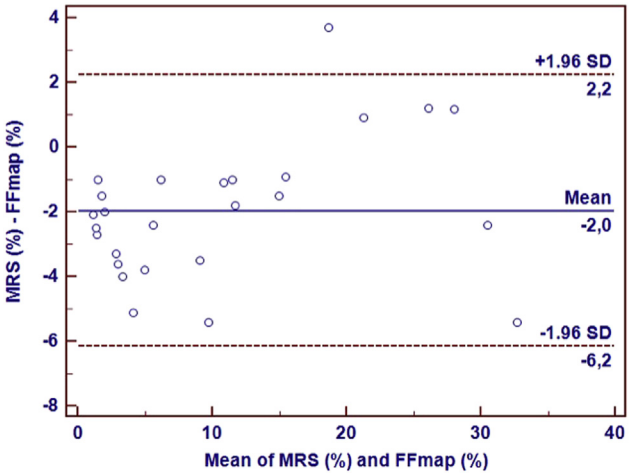

Figure 3. Bland-Altman plot representing the difference between liver fat fraction (FF; %) estimated with magnetic resonance spectroscopy (MRS) and mapping (measured by observer 1 at one time point) plotted against their means. Only one FF measurement was not within the ±1.96 standard deviation (SD) of the mean for both methods, but all FF measurements stayed within the upper maximum and lower minimum 95% limit of agreement.

within a short postprocessing time with excellent intra- and interobserver agreement. The cutoff value of 6.9% for the mapping method was found to have the best sensitivity and specificity to diagnose patients with and without liver fat deposition. Histological assessment of liver biopsy is considered the reference standard for the diagnosis of steatosis but its use for screening or follow-up studies remains impractical because of its invasive nature. Moreover, it is subjected to important sampling errors because liver steatosis is a heterogeneous process often associated with spared areas that may be related, among other reasons, to vascular abnormalities (17). The noninvasive quantification of liver fat has been made possible by the use of magnetic resonance imaging with either ^{1}H MRS or multiecho gradient-echo sequences. However, spectroscopy has limited spatial coverage and requires substantial expertise for its implementation and analysis, and the multiecho sequences (≥6 echos) require the use of equations with increasing complexity and additional analysis software to measure fat content (9,18,19). Recently, good agreement of fat fraction measurements between MRS and triple echo gradient-echo imaging over a wide range of fat content was reported (9). The FFM technique used in our study also showed very good correlation with MRS, although the correlation coefficient was lower than previous reports (∼0.98) (14). This may probably be explained by two factors: first, because of technical limitations at 1.5 T, we assumed a simplified fat spectrum consisting of a single methylene peak at 1.3 ppm (13), whereas gradient-echo magnetic resonance imaging includes signals from all fat peaks. Second, T2⋆ effect was corrected assuming a linear T2⋆ decay between the two IP echoes, as previously observed by Guiu et al. (14) However, to ensure that no bias from T2⋆ decay influenced our measurements, we used the first two closely spaced IP echo times to obtain the IP-corrected signal. These two IP echo times have superior signal-to-noise ratio and are less influenced by fat-fat interference. We are aware that the FFM technique does not solve the problem of fat-water ambiguity because subcutaneous fat will show values of 8–12%, when the real fat fraction is obtained subtracting this value from 100%. However, liver fat fractions higher than 50% are very uncommon in the liver parenchyma (8,9,11,15). The highest fat fraction measured in the present study was 35.4%. When performing visual assessment of the map, liver fat is hyperintense compared to the spleen, our internal reference. The spleen does not contain visible fat on magnetic resonance imaging (MRI) except in cases of lipid storage disorders and after administration of intravenous fat emulsions (14,20). Because splenic measurements obtained for all patients were consistently ≤1.5%, it allowed us to conclude about the good reproducibility of the technique.

The Bland-Altman plot showed that the fat fraction measurements for all patients, except one, were within ±4.2% of the mean difference of both methods. This is a fairly reasonable value considering that quantification of

liver fat by visual assessment on pathological specimens has broader grading limits (21). The median time spent for acquisition and postprocessing of ^{1}H MRS in our study was ~38 minutes, which can at least be partially explained by the lack of fully automated spectral analysis software. However, the mean time spent to produce and analyze FFM was only 5 min 35 seconds, which makes the technique a realistic choice to incorporate in a busy clinical setting.

Compared to previous studies that only assessed the agreement of the mapping technique with respect to an imaging gold standard (11,14), we have determined its cutoff value and intra- and interobserver reproducibility. Using 6.9% as a cutoff value can accurately distinguish patients with and without liver steatosis. Furthermore, in our work excellent intra- and interobserver reproducibility were observed and we believe that this is an additional reason to apply FFM as a potential biomarker for liver steatosis quantification. The clinical relevance of FFM must be considered especially in the setting of longitudinal population-based epidemiologic studies, because recent studies have reported a 5% prevalence of fatty liver in the general pediatric population, 38% in obese children, and 48% in children having type 2 diabetes (22).

Our study has limitations: first, steatosis quantification was not confirmed by histology because performing liver biopsy in asymptomatic patients is not ethically justified, and may be underrepresentative because only 1/50,000 of the organ is actually analyzed (21); second, the absence of liver iron overload was not histologically verified but it must be stressed that the present series was composed of patients only at risk for nonalcoholic fatty liver disease, without clinical or biological evidence of iron overload; third, we were not able to test the longitudinal reproducibility of FFM because each patient was submitted to a single MR session for each quantification technique.

In conclusion, FFM is a simple and accurate technique for liver steatosis quantification. Because it can be performed in a short time frame, it can potentially be included in routine liver studies dealing with this clinical problem, especially in the setting of large longitudinal population-based epidemiologic studies.

ACKNOWLEDGMENTS

The authors would like to acknowledge the radiology technicians Emílio Leal, Alda Pinto, Paulo Carvalho e Paula Marques, for performing the MRI and MRS examinations at the University Clinic of Radiology.

REFERENCES

1. Younossi ZM, Stepanova M, Afendy M, et al. Changes in the prevalence of the most common causes of chronic liver diseases in the United States from 1998 to 2008. Clin Gastroenterol Hepatol 2011; 9:524–530.
2. Chalasani N, Younossi Z, Lavine JE, et al. Liver disease: practice guideline by the American Association for the Study of Liver Diseases, American College of Gastroenterology, and the American Gastroenterological Association. Hepatology 2012; 55:2005–2023.
3. Pais R, Pascale A, Fedchuck L, et al. Progression from isolated steatosis to steatohepatitis and fibrosis in nonalcoholic fatty liver disease. Clin Res Hepatol Gastroenterol 2011; 35:23–28.
4. Won V, Wong G, Choi P, et al. Disease progression of non-alcoholic fatty liver disease: a prospective study with paired liver biopsies at 3 years. Gut 2010; 59:969–974.
5. Kim SR, Nakajima T, Ando K, et al. Two cases of nonalcoholic liver steatohepatitis developing from simple fatty liver. J Gastrointest Liver Dis 2009; 18:491–495.
6. Harrisson SA, Togerson S, Hayashi PH. The natural history of non alcoholic fatty liver disease: a clinical histopathological study. Am J Gastroenterol 2003; 98:2042–2047.
7. Brunt EM. Nonalcoholic fatty liver disease: what the pathologist can tell the clinician. Dig Dis 2012; 30:61–68.
8. Szczepaniak LS, Nurenberg P, Leonard D, et al. Magnetic resonance spectroscopy to measure hepatic triglyceride content: prevalence of hepatic steatosis in the general population. Am J Physiol Endocrinol Metab 2005; 288:E462–E468.
9. Yokoo T, Bydder M, Hamilton G, et al. Nonalcoholic fatty liver disease: diagnostic and fat-grading accuracy of low-flip-angle multiecho gradient-recalled-echo MR imaging at 1.5 T. Radiology 2009; 251: 67–76.
10. Yokoo T, Shiehmorteza M, Hamilton G, et al. Estimation of hepatic proton-density fat fraction by using MR imaging at 3.0 T. Radiology 2011; 258: 749–759.
11. Guiu B, Petit JM, Loffroy R, et al. Quantification of liver fat content: comparison of triple-echo chemical shift gradient-echo imaging and in vivo proton MR spectroscopy. Radiology 2009; 250:95–102.
12. d'Assignies G, Ruel M, Khiat A, et al. Noninvasive quantification of human liver steatosis using magnetic resonance methods. Eur Radiol 2009; 19: 2033–2040.
13. Reeder SB, Cruite I, Hamilton G, et al. Quantitative assessment of liver fat with magnetic resonance imaging and spectroscopy. JMRI 2011; 34: 729–749.
14. Guiu B, Loffroy R, Petit JM, et al. Mapping of liver fat with triple-echo gradient echo imaging: validation against 3.0-T proton MR spectroscopy. Eur Radiol 2009; 19:1786–1793.
15. Guiu B, Peti J-M, Capitan V, et al. Intravoxel incoherent motion diffusion-weighted imaging in nonalcoholic fatty liver disease: a 3.0-T MR study. Radiology 2012; 265:96–103.
16. Bland JM, Altman DG. Statistical methods for assessing agreement between two methods of clinical measurement. Lancet 1986; 1: 307–310.
17. Décarie P-O, Lepanto L, Billiard J-S, et al. Fatty liver deposition and sparing: a pictorial review. Insights Imaging 2011; 2:533–538.
18. Sirlin CB. Noninvasive imaging biomarkers for steatosis assessment. Liver Transpl 2009; 15:1389–1391.
19. Guiu B, Loffroy R, Ben Salem D, et al. Liver steatosis and in-phase/opposed-phase MR imaging: theory and clinical applications at 3 T. J Radiol 2007; 88:1845–1853.
20. Forbes GB. Splenic lipidosis after administration of intravenous fat emulsions. J Clin Pathol 1978; 31:765–771.
21. Brunt EM, Tiniakos DG. Histopathology of nonalcoholic fatty liver disease. World J Gastroenterol 2010; 16:5286–5296.
22. Stefan N, Kantartzis K, Häring H-U. Causes and metabolic consequences of fatty liver. Endocrinol Rev 2008; 29:939–960.